

Supplementary Information

Thermodynamic investigation of Ti doping in MgAl₂O₄ based on first-principles method

Yongseon Kim,¹ Jaehyuk Lim,² and Shinhoo Kang^{2}*

¹Department of Materials Science and Engineering, Inha University, Incheon, 402-751, Republic of Korea

²Department of Materials Science and Engineering, Seoul National University, Seoul, 151-742, Republic of Korea

Author E-mail: ys.kim@inha.ac.kr
lime819@snu.ac.kr
shinkang@snu.ac.kr

S1. Optimized cell parameters

The structure of each phase was optimized allowing full relaxation of the atomic positions and lattice vectors during the calculation. The optimized cell parameters of $2 \times 1 \times 1$ MgAl₂O₄:Ti supercells ($16.16 \times 8.08 \times 8.08$ Å³) which is composed of 112 atoms (48 metal atoms and 64 oxygen atoms) are presented in Table S1. The cell parameters were slightly different with doping type of Ti or associated defects but no significant difference was observed.

Doping types	Oxidation number of Ti	Optimized supercell parameters : a / b / c (Å)	Cell volume (Å ³)
❶ Ti _{Al} ' + Al _{Mg} •	+2	16.1747 / 8.0942 / 8.1019	1060.71
❷ Ti _{Mg} ×		16.1878 / 8.0951 / 8.0951	1060.80
❸ Ti _{Al} ×		16.2158 / 8.0965 / 8.0965	1063.00
❹ Ti _{Mg} • + Mg _{Al} '	+3	16.1870 / 8.0999 / 8.1000	1062.02
❺ Ti _{Al} • + Mg _{Al} '		16.1976 / 8.0993 / 8.0937	1061.81
❻ Ti _{Al} • + Mg _{Al} '	+4	16.2053 / 8.1013 / 8.1013	1063.57
❼ Ti _{Mg} •• + 2Mg _{Al} '		16.2189 / 8.1066 / 8.1066	1065.86

Table S1. Optimized cell parameters of $2 \times 1 \times 1$ MgAl₂O₄:Ti supercells.

S2. Selection of stable surface model

To examine the surface effects, DFT calculations for crystal models containing a (1 0 0) surface plane, which is a commonly observed surface from the morphology of a MgAl₂O₄ crystal, was performed. Like the bulk calculations, the basic crystal models were composed of 48 metal atoms and 64 oxygen atoms. After structure optimization of the equivalent bulk crystal model, a vacuum slab was inserted into the crystal to make two (1 0 0) surface planes inside the crystal, and the Ti and other point defects were set to be located at a similar distance from both of the (1 0 0) surfaces. The energy calculated at this stage, i.e., immediately after the formation of the surfaces by the insertion of a vacuum slab, was defined as the cleaving energy in this study. The position of the atoms near the surface was optimized so that they could adjust to the new environment of the surface. The energy change with this process was defined as the relaxation energy.^{s1,s2}

Determining the most stable surface configuration, i.e., termination of the crystal with the lowest surface

formation energy among the types of surface terminations,^{s3-s6} is the first task before examining the surface. Al/O and Mg layers repeat alternately along the [1 0 0] direction of MgAl₂O₄, and cleaving of the crystal is always polar resulting in asymmetric surfaces at both ends of the vacuum slab inserted inside the crystal (type III according to the classification of P. W. Tasker^{s3,s8}). Some studies have reported that making two surfaces symmetrical by moving some of the atoms from one side to another lowers the surface energy.

Al/O-terminated and Mg-terminated surfaces can be generated with the insertion of a vacuum slab between Al/O and Mg layer of MgAl₂O₄, as presented in Fig. S2. By applying the relaxation of the atomic position to one of the surfaces, the formation energy of the surface can be calculated using the following equation:^{s1}

$$\Delta E_{\text{surf}} = \Delta E_{\text{cleave}} + \Delta E_{\text{relax}} = \frac{1}{2}(E_{\text{cleaved}} - E_{\text{bulk}}) + (E_{\text{relaxed}} - E_{\text{cleaved}}),$$

where ΔE_{cleave} is the cleaving energy, which arises from bond breaking between atoms to create surfaces on either side of the vacuum slab, ΔE_{relax} indicates the energy change due to atomic relaxation to stable positions in the vicinity of the surface.

Two atomic layers from the surface were allowed to relax the position of atoms in this study: the relaxation of all atomic positions, which is general for the optimization of bulk crystal structure in DFT calculation, is not applicable. This is because the portion of atoms at a surface of the crystal model for surface calculation is large compared to the total number of atoms in the model due to limited model size, thus almost all atoms in the model would be affected by the surfaces. To avoid this situation it was necessary to divide the model into the bulk region in which the atoms are fixed at the position of optimized bulk crystal, and into the surface region in which the atomic position can be relaxed. We defined two outermost atomic layers as the surface region in this study.^{s1,s2}

The surfaces of non-polar cleaving, which could be obtained by moving 50% of O from the Al/O-terminated surface to Mg-terminated surface of the opposite side or 50% of Mg from the Mg-terminated surface to the Al/O surface, and the surface energies were examined. The energy of the Al/O (Mg), Mg (Al/O), Al/O_{0.5} (Mg), O_{0.5} (Mg), and Mg_{0.5} (Al/O) surfaces were calculated, and the results are shown in Table S1. In the expression of each surface, 0.5 means 50% coverage and () denotes the second layer from the outermost surface. The result indicates that the Mg_{0.5} (Al/O) surface is most stable with the lowest surface formation energy. Therefore, this type was used as a reference (1 0 0) surface for calculating the surface crystal models.

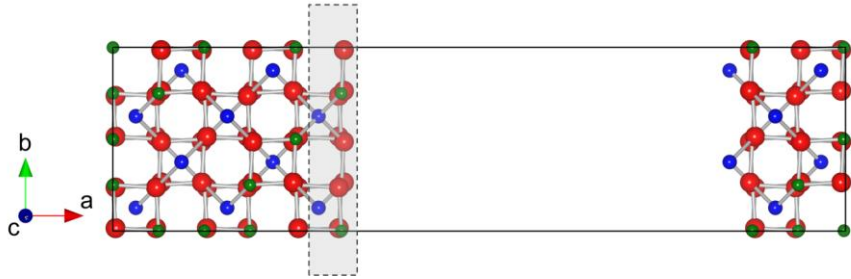


Fig. S2. Crystal model including the (1 0 0) surface: the crystal is cleaved between an Al/O layer and a Mg layer by the insertion of a vacuum slab. The atoms of the two surface layers were allowed to relax their position.

(100) surface planes	ΔE_{cleave} (eV nm $^{-2}$)	ΔE_{relax} (eV nm $^{-2}$)	ΔE_{surf} (eV nm $^{-2}$)
Al/O (Mg) surface	15.5072	-2.5092	12.9980
Mg (Al/O) surface	15.5072	-2.4644	13.0428
Al/O _{0.5} (Mg) surface	31.2992	-1.7940	29.5052
O _{0.5} (Mg) surface	31.2992	-8.2996	22.9996
Mg _{0.5} (Al/O)	13.3512	-3.2970	10.0542

Table S1. Cleaving energy, relaxation energy, and the surface formation energy calculated for various types of (1 0 0) surface of MgAl₂O₄.

S3. Oxidation state analysis of Ti

In this study, it was initially assumed that oxidation state of Ti could be changed more flexibly than that of any other point defects. To confirm the validity of the investigation, it was essential to examine whether this assumption is reasonable and the formal oxidation state of Ti determined on the basis is correct or not. For this purpose, the oxidation state of Ti was estimated from the magnetic moment obtained from the DFT calculation. Table S2 provides the originally assumed oxidation state of Ti, the magnetic moment of Ti, and the Kröger-Vink notation and oxidation state of Ti finally confirmed. Magnetic moment of Ti ions that were initially assumed to be Ti²⁺, Ti³⁺ and Ti⁴⁺ was over 1.6 μ_B , 0.89~0.91 μ_B , and 0 μ_B , respectively, indicating the initial assumption of Ti oxidation number was reasonable. The only exception was $\textcircled{2} \text{Ti}_{\text{Al}}^{\times} + 0.5\text{V}_0^{\bullet\bullet}$, which was initially assumed to be $\textcircled{2} \text{Ti}_{\text{Al}}' + 0.5\text{V}_0^{\bullet\bullet}$ but the magnetic moment of Ti in this type of defect combination was calculated to be 0.83 μ_B , rather close to Ti³⁺. This may indicate that the extra electron generated with

formation of oxygen vacancy would be trapped by the vacancy rather than reducing the Ti^{3+} ion to Ti^{2+} state.

Initial assumption	Magnetic moment (μ_B)	Final expression confirmed
① $\text{Ti}_{\text{Mg}}^{\times} (\text{Ti}^{2+})$	1.75	① $\text{Ti}_{\text{Mg}}^{\times} (\text{Ti}^{2+})$
② $\text{Ti}_{\text{Al}}' + \text{Al}_{\text{Mg}}^{\bullet} (\text{Ti}^{2+})$	1.62	② $\text{Ti}_{\text{Al}}' + \text{Al}_{\text{Mg}}^{\bullet} (\text{Ti}^{2+})$
③ $\text{Ti}_{\text{Al}}' + 0.5\text{V}_0^{\bullet\bullet} (\text{Ti}^{2+})$	0.83	③ $\text{Ti}_{\text{Al}}^{\times} + 0.5\text{V}_0^{\times} (\text{Ti}^{3+})$
④ $\text{Ti}_{\text{Mg}}^{\bullet} + \text{Mg}_{\text{Al}}' (\text{Ti}^{3+})$	0.90	④ $\text{Ti}_{\text{Mg}}^{\bullet} + \text{Mg}_{\text{Al}}' (\text{Ti}^{3+})$
⑤ $2\text{Ti}_{\text{Mg}}^{\bullet} + \text{V}_{\text{Mg}}'' (\text{Ti}^{3+})$	0.91	⑤ $2\text{Ti}_{\text{Mg}}^{\bullet} + \text{V}_{\text{Mg}}'' (\text{Ti}^{3+})$
⑥ $3\text{Ti}_{\text{Mg}}^{\bullet} + \text{V}_{\text{Al}}''' (\text{Ti}^{3+})$	0.91	⑥ $3\text{Ti}_{\text{Mg}}^{\bullet} + \text{V}_{\text{Al}}''' (\text{Ti}^{3+})$
⑦ $\text{Ti}_{\text{Al}}^{\times} (\text{Ti}^{3+})$	0.89	⑦ $\text{Ti}_{\text{Al}}^{\times} (\text{Ti}^{3+})$
⑧ $\text{Ti}_{\text{Mg}}^{\bullet\bullet} + 2\text{Mg}_{\text{Al}}' (\text{Ti}^{4+})$	0.00	⑧ $\text{Ti}_{\text{Mg}}^{\bullet\bullet} + 2\text{Mg}_{\text{Al}}' (\text{Ti}^{4+})$
⑨ $\text{Ti}_{\text{Mg}}^{\bullet\bullet} + \text{V}_{\text{Mg}}'' (\text{Ti}^{4+})$	0.00	⑨ $\text{Ti}_{\text{Mg}}^{\bullet\bullet} + \text{V}_{\text{Mg}}'' (\text{Ti}^{4+})$
⑩ $3\text{Ti}_{\text{Mg}}^{\bullet\bullet} + 2\text{V}_{\text{Al}}''' (\text{Ti}^{4+})$	0.00	⑩ $3\text{Ti}_{\text{Mg}}^{\bullet\bullet} + 2\text{V}_{\text{Al}}''' (\text{Ti}^{4+})$
⑪ $\text{Ti}_{\text{Al}}^{\bullet} + \text{Mg}_{\text{Al}}' (\text{Ti}^{4+})$	0.00	⑪ $\text{Ti}_{\text{Al}}^{\bullet} + \text{Mg}_{\text{Al}}' (\text{Ti}^{4+})$
⑫ $\text{Ti}_{\text{Al}}^{\bullet} + 0.5\text{V}_{\text{Mg}}'' (\text{Ti}^{4+})$	0.00	⑫ $\text{Ti}_{\text{Al}}^{\bullet} + 0.5\text{V}_{\text{Mg}}'' (\text{Ti}^{4+})$
⑬ $\text{Ti}_{\text{Al}}^{\bullet} + 1/3\text{V}_{\text{Al}}''' (\text{Ti}^{4+})$	0.00	⑬ $\text{Ti}_{\text{Al}}^{\bullet} + 1/3\text{V}_{\text{Al}}''' (\text{Ti}^{4+})$

Table S2. The Kröger-Vink notation of the 13 doping types and the oxidation state of Ti: initially assumed value and the final expression confirmed from the magnetic moment calculated by DFT.

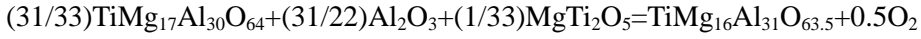
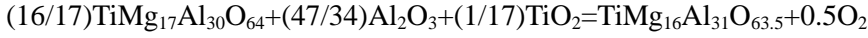
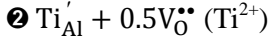
S4. Formation reaction and calculation of the fraction for each doping form

The following equation was derived and the fraction of each doping form was calculated, as discussed in the main body of the paper:

$$N_{(n)} \approx \exp\left(-\frac{\Delta E_{(n)}}{kT}\right)$$

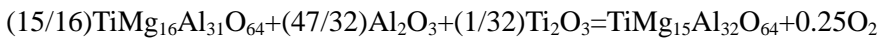
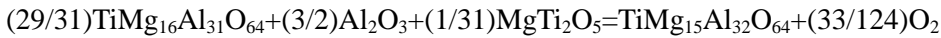
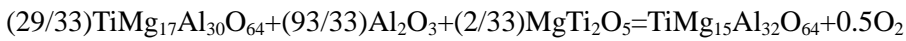
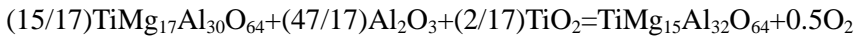
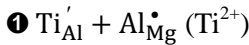
where $\Delta E_{(n)}$ is the formation energy of certain type (n-type) of doping model when it is formed from the most stable phases and can be calculated from the energy of products and reactants of the formation reaction by a DFT method. The most stable state under a given condition should be determined from the phase diagrams, which could be obtained by simulation, and the change of the phase diagram with temperature and pressure should also be considered. The reaction equation for calculating the formation energy, and the calculation result of the fraction as a function of a wide range of temperatures (column) and oxygen partial pressures (row)

for each doping form are given below. Different reaction equations should be applied when calculating the formation energy as the phase diagram changes with temperature or oxygen partial pressure. The conditions of the same formation reaction are marked as regions, and the equilibrium condition of H₂ (green line) and CO/CO₂ (blue line) is given together in the following data tables.



	1.00E-23	1.00E-21	1.00E-19	1.00E-17	1.00E-15	1.00E-13	1.00E-11	1.00E-09	1.00E-07	1.00E-05	1.00E-03	1.00E-01	1.00E+01	1.00E+03
100	3.28E-229	3.28E-230	3.28E-231	3.28E-232	3.28E-233	3.28E-234	3.28E-235	3.28E-236	3.28E-237	3.28E-238	3.28E-239	3.28E-240	3.28E-241	3.28E-242
200	4.64E-107	4.64E-108	4.64E-109	4.64E-110	4.64E-111	4.64E-112	4.64E-113	4.64E-114	4.64E-115	4.64E-116	4.64E-117	4.64E-118	4.64E-119	4.64E-120
300	3.30E-66	3.30E-67	3.30E-68	3.28E-69	3.28E-70	3.28E-71	3.28E-72	3.28E-73	3.28E-74	3.28E-75	3.28E-76	3.28E-77	3.28E-78	3.28E-79
400	1.02E-45	1.02E-46	1.02E-47	1.02E-48	1.02E-49	1.02E-50	1.02E-51	1.01E-52	1.01E-53	1.01E-54	1.01E-55	1.01E-56	1.01E-57	1.01E-58
500	2.19E-33	2.19E-34	2.19E-35	2.19E-36	2.19E-37	2.19E-38	2.19E-39	2.19E-40	2.19E-41	2.19E-42	2.19E-43	2.19E-44	2.19E-45	2.19E-46
600	3.90E-25	3.90E-26	3.90E-27	3.90E-28	3.90E-29	3.90E-30	3.90E-31	3.90E-32	3.90E-33	3.90E-34	3.89E-35	3.89E-36	3.89E-37	3.89E-38
700	3.19E-19	3.19E-20	3.19E-21	3.19E-22	3.19E-23	3.19E-24	3.19E-25	3.19E-26	3.19E-27	3.19E-28	3.19E-29	3.18E-30	3.18E-31	3.18E-32
800	8.97E-15	8.97E-16	8.97E-17	8.97E-18	8.97E-19	8.97E-20	8.97E-21	8.97E-22	8.97E-23	8.97E-24	8.97E-25	8.97E-26	8.96E-27	8.96E-28
900	2.67E-11	2.67E-12	2.67E-13	2.67E-14	2.67E-15	2.67E-16	2.67E-17	2.67E-18	2.67E-19	2.67E-20	2.67E-21	2.67E-22	2.67E-23	2.66E-24
1000	1.64E-08	1.64E-09	1.64E-10	1.64E-11	1.64E-12	1.64E-13	1.64E-14	1.64E-15	1.64E-16	1.64E-17	1.64E-18	1.64E-19	1.64E-20	1.64E-21
1100	1.54E-05	3.20E-07	3.20E-08	3.20E-09	3.20E-10	3.20E-11	3.20E-12	3.20E-13	3.20E-14	3.20E-15	3.20E-16	3.20E-17	3.20E-18	3.20E-19
1200	2.07E-04	6.55E-05	2.63E-06	2.66E-07	2.63E-08	2.63E-09	2.63E-10	2.63E-11	2.63E-12	2.63E-13	2.63E-14	2.63E-15	2.63E-16	2.63E-17
1300	1.88E-03	5.96E-04	1.88E-04	1.11E-05	4.11E-06	1.11E-07	1.11E-08	1.11E-09	1.11E-10	1.11E-11	1.11E-12	1.11E-13	1.11E-14	1.11E-15
1400	1.26E-02	3.98E-03	1.26E-03	2.79E-04	2.79E-05	2.79E-06	2.79E-07	2.79E-08	2.79E-09	2.79E-10	2.79E-11	2.79E-12	2.79E-13	2.79E-14
1500	6.55E-02	2.07E-02	6.55E-03	2.07E-03	4.60E-04	4.60E-05	4.60E-06	4.60E-07	4.60E-08	4.60E-09	4.60E-10	4.60E-11	4.60E-12	4.60E-13
1600	2.79E-01	8.82E-02	2.79E-02	8.82E-03	2.79E-03	5.40E-04	5.40E-05	5.40E-06	5.40E-07	5.40E-08	5.40E-09	5.40E-10	5.40E-11	5.40E-12
1700	1.01E+00	3.18E-01	1.01E-01	3.18E-02	1.01E-02	3.18E-03	4.78E-04	4.78E-05	4.78E-06	4.78E-07	4.78E-08	4.78E-09	4.78E-10	4.78E-11
1800	3.16E+00	9.98E-01	3.16E-01	9.98E-02	3.16E-02	9.98E-03	3.16E-03	3.34E-04	3.34E-05	3.34E-06	3.34E-07	3.34E-08	3.34E-09	3.34E-10

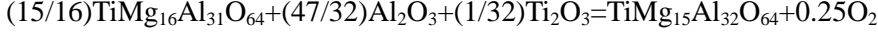
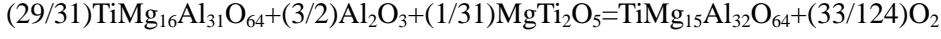
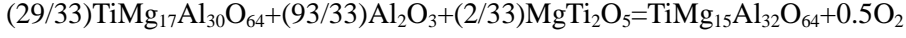
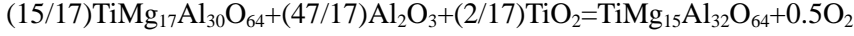
Table S3a. Equilibrium fraction of **② Ti_{Al}' + 0.5V_O• (Ti²⁺)** doping type calculated with respect to temperature and oxygen partial pressure. (The equilibrium condition of H₂ and CO/CO₂ atmosphere is marked with green and blue lines.)



	1.00E-23	1.00E-21	1.00E-19	1.00E-17	1.00E-15	1.00E-13	1.00E-11	1.00E-09	1.00E-07	1.00E-05	1.00E-03	1.00E-01	1.00E+01	1.00E+03
100	3.95E-263	3.95E-264	3.95E-265	3.95E-266	3.95E-267	3.95E-268	3.95E-269	3.95E-270	3.95E-271	3.95E-272	3.95E-273	3.95E-274	3.95E-275	3.95E-276
200	5.09E-124	5.09E-125	5.09E-126	5.09E-127	5.09E-128	5.09E-129	5.09E-130	5.09E-131	5.09E-132	5.09E-133	5.09E-134	5.09E-135	5.09E-136	5.09E-137
300	1.64E-77	1.64E-78	1.64E-79	1.62E-80	1.62E-81	1.62E-82	1.62E-83	1.62E-84	1.62E-85	1.62E-86	1.62E-87	1.62E-88	1.62E-89	1.62E-90
400	3.39E-54	3.39E-55	3.39E-56	3.39E-57	3.39E-58	3.39E-59	3.38E-60	3.36E-61	3.36E-62	3.36E-63	3.36E-64	3.36E-65	3.36E-66	3.36E-67
500	3.62E-40	3.62E-41	3.62E-42	3.62E-43	3.62E-44	3.62E-45	3.62E-46	3.62E-47	3.62E-48	3.60E-49	3.60E-50	3.60E-51	3.60E-52	3.60E-53
600	8.68E-31	8.68E-32	8.68E-33	8.68E-34	8.68E-35	8.68E-36	8.68E-37	8.68E-38	8.68E-39	8.68E-40	8.68E-41	8.64E-42	8.64E-43	8.64E-44
700	4.56E-24	4.56E-25	4.56E-26	4.56E-27	4.56E-28	4.56E-29	4.56E-30	4.56E-31	4.56E-32	4.56E-33	4.56E-34	4.56E-35	4.54E-36	4.54E-37
800	5.18E-19	5.18E-20	5.18E-21	5.18E-22	5.17E-23	5.17E-24	5.17E-25	5.17E-26	5.17E-27	5.17E-28	5.17E-29	5.17E-30	5.17E-31	5.16E-32
900	4.55E-15	4.55E-16	4.55E-17	4.55E-18	4.55E-19	4.55E-20	4.55E-21	4.55E-22	4.55E-23	4.55E-24	4.55E-25	4.55E-26	4.55E-27	4.54E-28
1000	6.66E-12	6.66E-13	6.66E-14	6.66E-15	6.66E-16	6.66E-17	6.66E-18	6.66E-19	6.66E-20	6.66E-21	6.66E-22	6.66E-23	6.66E-24	6.66E-25
1100	2.64E-09	2.64E-10	2.64E-11	2.64E-12	2.64E-13	2.64E-14	2.64E-15	2.64E-16	2.64E-17	2.64E-18	2.64E-19	2.64E-20	2.64E-21	2.64E-22
1200	3.14E-07	3.93E-08	3.93E-09	3.98E-10	3.93E-11	3.93E-12	3.93E-13	3.93E-14	3.93E-15	3.93E-16	3.93E-17	3.93E-18	3.93E-19	3.93E-20
1300	5.20E-06	1.53E-06	2.74E-07	2.74E-08	2.74E-09	2.74E-10	2.74E-11	2.74E-12	2.74E-13	2.74E-14	2.74E-15	2.74E-16	2.74E-17	2.74E-18
1400	5.61E-05	1.70E-05	5.01E-06	1.06E-06	1.06E-07	1.06E-08	1.06E-09	1.06E-10	1.06E-11	1.06E-12	1.06E-13	1.06E-14	1.06E-15	1.06E-16
1500	4.20E-04	1.33E-04	4.07E-05	1.20E-05	2.52E-06	2.52E-07	2.52E-08	2.52E-09	2.52E-10	2.52E-11	2.52E-12	2.52E-13	2.52E-14	2.52E-15
1600	2.45E-03	7.75E-04	2.45E-04	7.53E-05	2.21E-05	4.10E-06	4.10E-07	4.10E-08	4.10E-09	4.10E-10	4.10E-11	4.10E-12	4.10E-13	4.10E-14
1700	1.17E-02	3.69E-03	1.17E-03	3.69E-04	1.13E-04	3.30E-05	4.83E-06	4.83E-07	4.83E-08	4.83E-09	4.83E-10	4.83E-11	4.83E-12	4.83E-13
1800	4.69E-02	1.48E-02	4.69E-03	1.48E-03	4.69E-04	1.41E-04	4.14E-05	4.36E-06	4.36E-07	4.36E-08	4.36E-09	4.36E-10	4.36E-11	4.36E-12

Table S3b. Equilibrium fraction of ① $Ti_{Al}^{'} + Al_{Mg}^{\bullet}$ doping type calculated with respect to temperature and oxygen partial pressure. (The equilibrium condition of H_2 and CO/CO_2 atmosphere is marked with green and blue lines.)

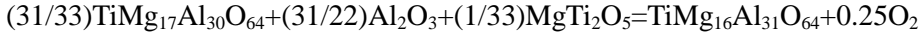
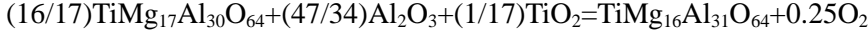
① $Ti_{Mg}^{X_g} (Ti^{2+})$



	1.00E-23	1.00E-21	1.00E-19	1.00E-17	1.00E-15	1.00E-13	1.00E-11	1.00E-09	1.00E-07	1.00E-05	1.00E-03	1.00E-01	1.00E+01	1.00E+03
100	2.40E-267	2.40E-268	2.40E-269	2.40E-270	2.40E-271	2.40E-272	2.40E-273	2.40E-274	2.40E-275	2.40E-276	2.40E-277	2.40E-278	2.40E-279	2.40E-280
200	3.97E-126	3.97E-127	3.97E-128	3.97E-129	3.97E-130	3.97E-131	3.97E-132	3.97E-133	3.97E-134	3.97E-135	3.97E-136	3.97E-137	3.97E-138	3.97E-139
300	6.43E-79	6.43E-80	6.43E-81	6.37E-82	6.37E-83	6.37E-84	6.37E-85	6.37E-86	6.37E-87	6.37E-88	6.37E-89	6.37E-90	6.37E-91	6.37E-92
400	2.99E-55	2.99E-56	2.99E-57	2.99E-58	2.99E-59	2.99E-60	2.99E-61	2.96E-62	2.96E-63	2.96E-64	2.96E-65	2.96E-66	2.96E-67	2.96E-68
500	5.19E-41	5.19E-42	5.19E-43	5.19E-44	5.19E-45	5.19E-46	5.19E-47	5.19E-48	5.19E-49	5.16E-50	5.16E-51	5.16E-52	5.16E-53	5.16E-54
600	1.72E-31	1.72E-32	1.72E-33	1.72E-34	1.72E-35	1.72E-36	1.72E-37	1.72E-38	1.72E-39	1.72E-40	1.72E-41	1.71E-42	1.71E-43	1.71E-44
700	1.14E-24	1.14E-25	1.14E-26	1.14E-27	1.14E-28	1.14E-29	1.14E-30	1.14E-31	1.14E-32	1.14E-33	1.14E-34	1.14E-35	1.13E-36	1.13E-37
800	1.54E-19	1.54E-20	1.54E-21	1.54E-22	1.54E-23	1.54E-24	1.54E-25	1.54E-26	1.54E-27	1.54E-28	1.54E-29	1.54E-30	1.54E-31	1.53E-32
900	4.55E-15	4.55E-16	4.55E-17	4.55E-18	4.55E-19	4.55E-20	4.55E-21	4.55E-22	4.55E-23	4.55E-24	4.55E-25	4.55E-26	4.54E-27	4.54E-28
1000	2.52E-12	2.52E-13	2.52E-14	2.52E-15	2.52E-16	2.52E-17	2.52E-18	2.52E-19	2.52E-20	2.52E-21	2.52E-22	2.52E-23	2.52E-24	2.52E-25
1100	1.09E-09	1.09E-10	1.09E-11	1.09E-12	1.09E-13	1.09E-14	1.09E-15	1.09E-16	1.09E-17	1.09E-18	1.09E-19	1.09E-20	1.09E-21	1.09E-22
1200	1.40E-07	1.75E-08	1.75E-09	1.75E-10	1.75E-11	1.75E-12	1.75E-13	1.75E-14	1.75E-15	1.75E-16	1.75E-17	1.75E-18	1.75E-19	1.75E-20
1300	2.46E-06	7.23E-07	1.30E-07	1.30E-08	1.30E-09	1.30E-10	1.30E-11	1.30E-12	1.30E-13	1.30E-14	1.30E-15	1.30E-16	1.30E-17	1.30E-18
1400	2.81E-05	8.52E-06	2.50E-06	5.28E-07	5.28E-08	5.28E-09	5.28E-10	5.28E-11	5.28E-12	5.28E-13	5.27E-14	5.27E-15	5.27E-16	5.27E-17
1500	2.20E-04	6.94E-05	2.13E-05	6.26E-06	1.32E-06	1.32E-07	1.32E-08	1.32E-09	1.32E-10	1.32E-11	1.32E-12	1.32E-13	1.32E-14	1.32E-15
1600	1.34E-03	4.22E-04	1.34E-04	4.10E-05	1.20E-05	2.23E-06	2.23E-07	2.23E-08	2.23E-09	2.23E-10	2.23E-11	2.23E-12	2.23E-13	2.23E-14
1700	6.59E-03	2.08E-03	6.59E-04	2.08E-04	6.36E-05	1.87E-05	1.73E-06	2.73E-07	2.73E-08	2.73E-09	2.73E-10	2.73E-11	2.73E-12	2.73E-13
1800	2.74E-02	8.65E-03	2.74E-03	8.65E-04	2.74E-04	8.22E-05	2.41E-05	2.54E-06	2.54E-07	2.54E-08	2.54E-09	2.54E-10	2.54E-11	2.54E-12

Table S3c. Equilibrium fraction of ① $Ti_{Mg}^{X_g}$ doping type calculated with respect to temperature and oxygen partial pressure. (The equilibrium condition of H_2 and CO/CO_2 atmosphere is marked with green and blue lines.)

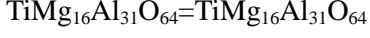
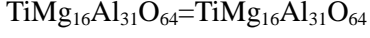
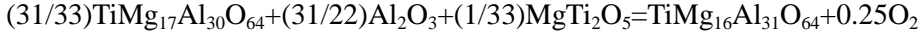
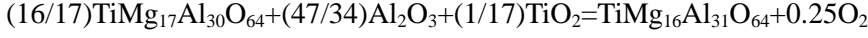
③ $\text{Ti}_{\text{Al}}^{\times} (\text{Ti}^{3+})$



	1.00E-23	1.00E-21	1.00E-19	1.00E-17	1.00E-15	1.00E-13	1.00E-11	1.00E-09	1.00E-07	1.00E-05	1.00E-03	1.00E-01	1.00E+01	1.00E+03
100	3.04E-92	9.62E-93	3.04E-93	9.62E-94	3.04E-94	9.62E-95	3.04E-95	9.62E-96	3.04E-96	9.62E-97	3.04E-97	1.44E-97	3.04E-98	9.62E-99
200	1.57E-42	4.96E-43	1.57E-43	4.96E-44	1.57E-44	4.96E-45	1.57E-45	4.96E-46	1.57E-46	4.96E-47	1.57E-47	7.42E-48	1.57E-48	4.96E-49
300	6.84E-26	2.16E-26	6.84E-27	2.15E-27	6.81E-28	2.15E-28	6.81E-29	2.15E-29	6.81E-30	2.15E-30	6.81E-31	3.22E-31	6.81E-32	2.15E-32
400	1.53E-17	4.85E-18	1.53E-18	4.85E-19	1.53E-19	4.85E-20	1.53E-20	4.83E-21	1.53E-21	4.83E-22	1.53E-22	7.23E-23	1.53E-23	4.83E-24
500	1.65E-12	5.20E-13	1.65E-13	5.20E-14	1.65E-14	5.20E-15	1.65E-15	5.20E-16	1.65E-16	5.19E-17	1.64E-17	7.76E-18	1.64E-18	5.19E-19
600	3.83E-09	1.21E-09	3.83E-10	1.21E-10	3.83E-11	1.21E-11	3.83E-12	1.21E-12	3.83E-13	1.21E-13	3.83E-14	1.81E-14	3.82E-15	1.21E-15
700	9.97E-07	3.15E-07	9.97E-08	3.15E-08	9.97E-09	3.15E-09	9.97E-10	3.15E-10	9.97E-11	3.15E-11	9.97E-12	4.71E-12	9.95E-13	3.15E-13
800	6.57E-05	2.08E-05	6.57E-06	2.08E-06	6.57E-07	2.08E-07	6.57E-08	2.08E-08	6.57E-09	2.08E-09	6.57E-10	3.11E-10	6.57E-11	2.07E-11
900	4.73E-03	5.48E-04	1.73E-04	5.48E-05	1.73E-05	5.48E-06	1.73E-06	5.48E-07	1.73E-07	5.48E-08	1.73E-08	8.19E-09	1.73E-09	5.47E-10
1000	2.40E-02	5.95E-03	2.40E-03	7.59E-04	2.40E-04	7.59E-05	2.40E-05	7.59E-06	2.40E-06	7.59E-07	2.40E-07	1.14E-07	2.40E-08	7.59E-09
1100	2.08E-01	6.59E-02	2.08E-02	6.59E-03	2.08E-03	6.59E-04	2.08E-04	6.59E-05	2.08E-05	6.59E-06	2.08E-06	9.85E-07	2.08E-07	6.59E-08
1200	ref.	4.02E-01	1.27E-01	4.02E-02	1.27E-02	4.02E-03	1.27E-03	4.02E-04	1.27E-04	4.02E-05	1.27E-05	6.01E-06	1.27E-06	4.02E-07
1300	ref.	ref.	5.91E-01	1.87E-01	5.91E-02	1.87E-02	5.91E-03	1.87E-03	5.91E-04	1.87E-04	5.91E-05	2.79E-05	5.91E-06	1.87E-06
1400	ref.	ref.	ref.	7.02E-01	2.22E-01	7.02E-02	2.22E-02	7.02E-03	2.22E-03	7.02E-04	2.22E-04	1.05E-04	2.22E-05	7.02E-06
1500	ref.	ref.	ref.	ref.	7.03E-01	2.22E-01	7.03E-02	2.22E-02	7.03E-03	2.22E-03	7.03E-04	3.32E-04	7.03E-05	2.22E-05
1600	ref.	ref.	ref.	ref.	ref.	6.12E-01	1.93E-01	6.12E-02	1.93E-02	6.12E-03	1.93E-03	9.15E-04	1.93E-04	6.12E-05
1700	ref.	ref.	ref.	ref.	ref.	ref.	7.75E-01	1.50E-01	4.75E-02	1.50E-02	4.75E-03	2.25E-03	4.75E-04	1.50E-04
1800	ref.	3.35E-01	1.06E-01	3.35E-02	1.06E-02	5.00E-03	1.06E-03	3.35E-04						

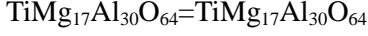
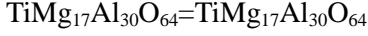
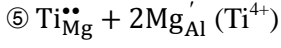
Table S3d. Equilibrium fraction of ③ $\text{Ti}_{\text{Al}}^{\times}$ doping type calculated with respect to temperature and oxygen partial pressure. (The equilibrium condition of H₂ and CO/CO₂ atmosphere is marked with green and blue lines.)

② $\text{Ti}_{\text{Mg}}^{\bullet} + \text{Mg}_{\text{Al}}' (\text{Ti}^{3+})$



	1.00E-23	1.00E-21	1.00E-19	1.00E-17	1.00E-15	1.00E-13	1.00E-11	1.00E-09	1.00E-07	1.00E-05	1.00E-03	1.00E-01	1.00E+01	1.00E+03
100	1.57E-122	4.96E-123	1.57E-123	4.96E-124	1.57E-124	4.96E-125	1.57E-125	4.96E-126	1.57E-126	4.96E-127	1.57E-127	4.96E-128	1.57E-128	4.96E-129
200	1.13E-57	3.56E-58	1.13E-58	3.56E-59	1.13E-59	3.56E-60	1.13E-60	3.56E-61	1.13E-61	3.56E-62	1.13E-62	3.56E-63	1.13E-63	3.56E-64
300	5.49E-36	1.74E-36	5.49E-37	1.73E-37	5.46E-38	1.73E-38	5.46E-39	1.73E-39	5.46E-40	1.73E-40	5.46E-41	1.73E-41	5.46E-42	1.73E-42
400	4.11E-25	1.30E-25	4.11E-26	1.30E-26	4.11E-27	1.30E-27	4.11E-28	1.30E-28	4.10E-29	1.30E-29	4.10E-30	1.30E-30	4.10E-31	1.30E-31
500	1.44E-18	4.56E-19	1.44E-19	4.56E-20	1.44E-20	4.56E-21	1.44E-21	4.56E-22	1.44E-22	4.54E-23	1.44E-23	4.54E-24	1.44E-24	4.54E-25
600	3.43E-14	1.09E-14	3.43E-15	1.09E-15	3.43E-16	1.09E-16	3.43E-17	1.09E-17	3.43E-18	1.09E-18	3.43E-19	1.08E-19	3.42E-20	1.08E-20
700	4.70E-11	1.49E-11	4.70E-12	1.49E-12	4.70E-13	1.49E-13	4.70E-14	1.49E-14	4.70E-15	1.49E-15	4.70E-16	1.49E-16	4.69E-17	1.48E-17
800	1.08E-08	3.40E-09	1.08E-09	3.40E-10	1.08E-10	3.40E-11	1.08E-11	3.40E-12	1.08E-12	3.40E-13	1.08E-13	3.40E-14	1.08E-14	3.39E-15
900	7.47E-07	2.36E-07	7.47E-08	2.36E-08	7.47E-09	2.36E-09	7.47E-10	2.36E-10	7.47E-11	2.36E-11	7.47E-12	2.36E-12	7.47E-13	2.36E-13
1000	2.25E-05	7.0E-06	2.25E-06	7.10E-07	2.25E-07	7.10E-08	2.25E-08	7.10E-09	2.25E-09	7.10E-10	2.25E-10	7.10E-11	2.25E-11	7.10E-12
1100	3.67E-04	1.16E-04	3.67E-05	1.16E-05	3.67E-06	1.16E-06	3.67E-07	1.16E-07	3.67E-08	1.16E-08	3.67E-09	1.16E-09	3.67E-10	1.16E-10
1200	2.99E-03	1.20E-03	3.80E-04	1.20E-04	3.80E-05	1.20E-05	3.80E-06	1.20E-06	3.80E-07	1.20E-07	3.80E-08	1.20E-08	3.80E-09	1.20E-09
1300	4.68E-03	4.68E-03	2.77E-03	8.75E-04	2.77E-04	8.75E-05	2.77E-05	8.75E-06	2.77E-06	8.74E-07	2.77E-07	8.74E-08	2.77E-08	8.74E-09
1400	6.86E-03	6.86E-03	6.86E-03	4.82E-03	1.52E-03	4.82E-04	1.52E-04	4.82E-05	1.52E-05	4.82E-06	1.52E-06	4.82E-07	1.52E-07	4.82E-08
1500	9.57E-03	9.57E-03	9.57E-03	9.57E-03	6.72E-03	2.43E-03	6.72E-04	2.13E-04	6.72E-05	2.13E-05	6.72E-06	2.13E-06	6.72E-07	2.13E-07
1600	1.28E-02	1.28E-02	1.28E-02	1.28E-02	1.28E-02	7.83E-03	2.48E-03	7.83E-04	2.48E-04	7.83E-05	2.48E-05	7.83E-06	2.48E-06	7.83E-07
1700	1.65E-02	1.65E-02	1.65E-02	1.65E-02	1.65E-02	1.65E-02	1.85E-03	2.48E-03	7.85E-04	2.48E-04	7.85E-05	2.48E-05	7.85E-06	2.48E-06
1800	2.08E-02	6.95E-03	2.20E-03	6.95E-04	2.20E-04	6.95E-05	2.20E-05	6.95E-06						

Table S3e. Equilibrium fraction of ② $\text{Ti}_{\text{Mg}}^{\bullet\bullet} + \text{Mg}_{\text{Al}}'$ doping type calculated with respect to temperature and oxygen partial pressure. (The equilibrium condition of H_2 and CO/CO_2 atmosphere is marked with green and blue lines.)



	1.00E-23	1.00E-21	1.00E-19	1.00E-17	1.00E-15	1.00E-13	1.00E-11	1.00E-09	1.00E-07	1.00E-05	1.00E-03	1.00E-01	1.00E+01	1.00E+03
100	4.37E-12													
200	2.09E-06													
300	1.63E-04													
400	1.45E-03													
500	5.35E-03													
600	1.28E-02													
700	2.38E-02													
800	5.47E-02													
900	7.31E-02													
1000	9.27E-02													
1100	1.13E-01													
1200	1.34E-01													
1300	1.54E-01													
1400	1.75E-01													
1500	1.95E-01													
1600	2.15E-01													
1700	2.34E-01													
1800	2.54E-01													

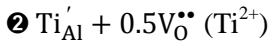
Table S3f. Equilibrium fraction of ⑤ $\text{Ti}_{\text{Mg}}^{\bullet\bullet} + 2\text{Mg}_{\text{Al}}'$ doping type calculated with respect to temperature and oxygen partial pressure. (The equilibrium condition of H_2 and CO/CO_2 atmosphere is marked with green and blue lines.)

S5. Errors of quantitative calculation model

Several error factors in the derivation of eq. 4 may need to be mentioned: First, the mixing entropy of the other phases participating in the formation reaction of a certain doping form was not considered. For example, Al_2O_3 , and TiO_2 were involved in the reaction of eq. 3 but the change in mixing entropy related to their generation or consumption is ignored. However, the effects of this error factor does not appear to be significant; considering that the domains of these phases would be large (enough often to be detected by XRD) compared to the unit of doping model crystals, the mixing entropy related to them is expected to be of minor influence. Another error may arise from the fact that this study only considered binary mixing of doping forms, i.e., a certain doping model of interest and the most stable doping form under a given condition. Mixing of the third, fourth, etc. type of doping should be included in principle. However, considering that the fraction of most of the doping forms except the most stable one is very small, this error term is still expected to be negligible compared to the formation Gibbs free energy.

S6. Calculation of the fraction for each doping form using surface model

Fraction of each doping form was calculated and the data is presented in S4. The same calculation, but with the surface crystal model, was performed to examine the surface effect and the data is given in this section. Each doping form is positioned near the surface; therefore, the data provide information on the fraction in the surface region, whereas the data in S4 section provides information in the bulk region. Single crystals or powders with a relatively large particle size may be interpreted with bulk models of S4 section, but the surface character of this section would be reflected more for nanoparticles or thin films with a high specific surface area. The particle size of Ti doped MgAl_2O_4 may be optimized for applications based on a simulation of the combination of the bulk (S4) and surface (S6) characters as a function of the particle size.



	1.00E-23	1.00E-21	1.00E-19	1.00E-17	1.00E-15	1.00E-13	1.00E-11	1.00E-09	1.00E-07	1.00E-05	1.00E-03	1.00E-01	1.00E+01	1.00E+03
100	0.00E+00													
200	7.99E-161	7.99E-162	7.99E-163	7.99E-164	7.99E-165	7.99E-166	7.99E-167	7.99E-168	7.99E-169	7.99E-170	7.99E-171	7.99E-172	7.99E-173	7.99E-174
300	2.12E-102	2.12E-103	2.12E-104	4.71E-105	4.71E-106	4.71E-107	4.71E-108	4.71E-109	4.71E-110	4.71E-111	4.71E-112	4.71E-113	4.71E-114	4.71E-115
400	7.30E-73	7.30E-74	7.30E-75	7.30E-76	7.30E-77	7.30E-78	7.30E-79	1.33E-79	1.33E-80	1.33E-81	1.33E-82	1.33E-83	1.33E-84	1.33E-85
500	4.23E-55	4.23E-56	4.23E-57	4.23E-58	4.23E-59	4.23E-60	4.23E-61	4.23E-62	4.23E-63	6.83E-64	6.83E-65	6.83E-66	6.83E-67	6.83E-68
600	3.12E-43	3.12E-44	3.12E-45	3.12E-46	3.12E-47	3.12E-48	3.12E-49	3.12E-50	3.12E-51	3.12E-52	4.66E-53	4.66E-54	4.66E-55	4.66E-56
700	9.83E-35	9.83E-36	9.83E-37	9.83E-38	9.83E-39	9.83E-40	9.82E-41	9.82E-42	9.82E-43	9.82E-44	9.82E-45	1.38E-45	1.38E-46	1.38E-47
800	2.40E-28	2.40E-29	2.40E-30	2.40E-31	2.40E-32	2.40E-33	2.40E-34	2.40E-35	2.40E-36	2.40E-37	2.40E-38	2.40E-39	3.24E-40	3.24E-41
900	2.30E-20	2.30E-21	2.30E-22	2.30E-23	2.30E-24	2.30E-25	2.30E-26	2.30E-27	2.30E-28	2.30E-29	2.30E-30	2.30E-31	2.30E-32	2.30E-33
1000	2.28E-19	2.28E-20	2.28E-21	2.28E-22	2.28E-23	2.28E-24	2.28E-25	2.28E-26	2.28E-27	2.28E-28	2.28E-29	2.28E-30	2.28E-31	2.89E-32
1100	1.28E-11	4.31E-17	4.31E-18	4.31E-19	4.31E-20	4.31E-21	4.31E-22	4.31E-23	4.31E-24	4.31E-25	4.31E-26	4.31E-27	4.31E-28	4.31E-29
1200	5.55E-10	1.76E-10	2.35E-15	2.35E-16	2.35E-17	2.35E-18	2.35E-19	2.35E-20	2.35E-21	2.35E-22	2.35E-23	2.35E-24	2.35E-25	2.35E-26
1300	1.36E-08	4.29E-09	1.36E-09	4.95E-14	4.95E-15	4.95E-16	4.95E-17	4.95E-18	4.95E-19	4.95E-20	4.95E-21	4.95E-22	4.95E-23	4.95E-24
1400	2.11E-07	6.67E-08	2.11E-08	4.90E-12	4.90E-13	4.90E-14	4.90E-15	4.90E-16	4.90E-17	4.90E-18	4.90E-19	4.90E-20	4.90E-21	4.90E-22
1500	2.29E-06	7.23E-07	2.29E-07	7.23E-08	2.66E-11	2.66E-12	2.66E-13	2.66E-14	2.66E-15	2.66E-16	2.66E-17	2.66E-18	2.66E-19	2.66E-20
1600	1.85E-05	5.85E-06	1.85E-06	5.85E-07	1.85E-07	8.83E-11	8.83E-12	8.83E-13	8.83E-14	8.83E-15	8.83E-16	8.83E-17	8.83E-18	8.83E-19
1700	1.17E-04	3.71E-05	1.17E-05	3.71E-06	1.17E-06	3.71E-07	1.96E-10	1.96E-11	1.96E-12	1.96E-13	1.96E-14	1.96E-15	1.96E-16	1.96E-17
1800	6.10E-04	1.93E-04	6.10E-05	1.93E-05	6.10E-06	1.93E-06	6.10E-07	3.10E-10	3.10E-11	3.10E-12	3.10E-13	3.10E-14	3.10E-15	3.10E-16

Table S4a. Equilibrium fraction of $\textcircled{2} \text{ Ti}_{\text{Al}}' + 0.5\text{V}_0^{\bullet\bullet}$ doping type calculated with respect to temperature and oxygen partial pressure using surface model. (The equilibrium condition of H₂ and CO/CO₂ atmosphere is marked with green and blue lines.)



	1.00E-23	1.00E-21	1.00E-19	1.00E-17	1.00E-15	1.00E-13	1.00E-11	1.00E-09	1.00E-07	1.00E-05	1.00E-03	1.00E-01	1.00E+01	1.00E+03
100	0.00E+00													
200	1.03E-164	1.03E-165	1.03E-166	1.03E-167	1.03E-168	1.03E-169	1.03E-170	1.03E-171	1.03E-172	1.03E-173	1.03E-174	1.03E-175	1.03E-176	1.03E-177
300	2.43E-105	2.43E-106	2.43E-107	1.20E-107	1.20E-108	1.20E-109	1.20E-110	1.20E-111	1.20E-112	1.20E-113	1.20E-114	1.20E-115	1.20E-116	1.20E-117
400	4.55E-75	4.55E-76	4.55E-77	4.55E-78	4.55E-79	4.55E-80	4.55E-81	1.51E-81	1.51E-82	1.51E-83	1.51E-84	1.51E-85	1.51E-86	1.51E-87
500	7.27E-57	7.27E-58	7.27E-59	7.26E-60	7.26E-61	7.26E-62	7.26E-63	7.26E-64	7.26E-65	1.90E-65	1.90E-66	1.90E-67	1.90E-68	1.90E-69
600	1.06E-44	1.06E-45	1.06E-46	1.06E-47	1.06E-48	1.06E-49	1.06E-50	1.06E-51	1.06E-52	1.06E-53	1.06E-54	2.35E-55	2.35E-56	2.35E-57
700	5.39E-36	5.39E-37	5.39E-38	5.39E-39	5.39E-40	5.39E-41	5.39E-42	5.39E-43	5.39E-44	5.39E-45	5.39E-46	5.39E-47	1.07E-47	1.07E-48
800	1.90E-29	1.90E-30	1.90E-31	1.90E-32	1.90E-33	1.90E-34	1.90E-35	1.90E-36	1.90E-37	1.90E-38	1.90E-39	1.90E-40	1.90E-41	3.46E-42
900	2.41E-84	2.41E-24	2.41E-25	2.41E-26	2.41E-27	2.41E-28	2.41E-29	2.41E-30	2.41E-31	2.41E-32	2.41E-33	2.41E-34	2.41E-35	2.41E-36
1000	2.98E-20	2.98E-21	2.98E-22	2.98E-23	2.98E-24	2.98E-25	2.98E-26	2.98E-27	2.98E-28	2.98E-29	2.98E-30	2.98E-31	2.98E-32	2.98E-33
1100	6.79E-17	6.79E-18	6.79E-19	6.79E-20	6.79E-21	6.79E-22	6.79E-23	6.79E-24	6.79E-25	6.79E-26	6.79E-27	6.79E-28	6.79E-29	6.79E-30
1200	6.19E-11	4.33E-15	4.33E-16	4.33E-17	4.33E-18	4.33E-19	4.33E-20	4.33E-21	4.33E-22	4.33E-23	4.33E-24	4.33E-25	4.33E-26	4.33E-27
1300	1.98E-09	5.81E-10	1.04E-13	1.04E-14	1.04E-15	1.04E-16	1.04E-17	1.04E-18	1.04E-19	1.04E-20	1.04E-21	1.04E-22	1.04E-23	1.04E-24
1400	4.56E-08	1.14E-08	1.34E-09	1.15E-12	1.15E-13	1.15E-14	1.15E-15	1.15E-16	1.15E-17	1.15E-18	1.15E-19	1.15E-20	1.15E-21	1.15E-22
1500	5.48E-07	1.73E-07	4.43E-08	1.30E-08	6.86E-12	6.86E-13	6.86E-14	6.86E-15	6.86E-16	6.86E-17	6.86E-18	6.86E-19	6.86E-20	6.86E-21
1600	4.85E-06	1.53E-06	4.85E-07	1.25E-07	3.68E-08	2.48E-11	2.48E-12	2.48E-13	2.48E-14	2.48E-15	2.48E-16	2.48E-17	2.48E-18	2.48E-19
1700	3.33E-05	1.05E-05	3.33E-06	1.05E-06	2.73E-07	8.02E-08	5.93E-11	5.93E-12	5.93E-13	5.93E-14	5.93E-15	5.93E-16	5.93E-17	5.93E-18
1800	1.85E-04	5.86E-05	1.85E-05	5.86E-06	1.85E-06	4.78E-07	1.40E-07	1.00E-10	1.00E-11	1.00E-12	1.00E-13	1.00E-14	1.00E-15	1.00E-16

Table S4b. Equilibrium fraction of $\textcircled{1} \text{ Ti}_{\text{Al}}' + \text{Al}_{\text{Mg}}^{\bullet}$ doping type calculated with respect to temperature and oxygen partial pressure using surface model. (The equilibrium condition of H₂ and CO/CO₂ atmosphere is marked with green and blue lines.)

① $\text{Ti}_{\text{Mg}}^{\times} (\text{Ti}^{2+})$

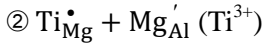
	1.00E-23	1.00E-21	1.00E-19	1.00E-17	1.00E-15	1.00E-13	1.00E-11	1.00E-09	1.00E-07	1.00E-05	1.00E-03	1.00E-01	1.00E+01	1.00E+03
100	0.00E+00													
200	1.26E-182	1.26E-183	1.26E-184	1.26E-185	1.26E-186	1.26E-187	1.26E-188	1.26E-189	1.26E-190	1.26E-191	1.26E-192	1.26E-193	1.26E-194	1.26E-195
300	2.78E-117	2.78E-118	2.78E-119	1.38E-119	1.38E-120	1.38E-121	1.38E-122	1.38E-123	1.38E-124	1.38E-125	1.38E-126	1.38E-127	1.38E-128	1.38E-129
400	5.04E-84	5.04E-85	5.04E-86	5.04E-87	5.04E-88	5.04E-89	5.04E-90	1.67E-90	1.67E-91	1.67E-92	1.67E-93	1.67E-94	1.67E-95	1.67E-96
500	4.98E-64	4.98E-65	4.98E-66	4.98E-67	4.98E-68	4.98E-69	4.98E-70	4.98E-71	4.98E-72	1.30E-72	1.30E-73	1.30E-74	1.30E-75	1.30E-76
600	1.13E-50	1.13E-51	1.13E-52	1.13E-53	1.13E-54	1.13E-55	1.13E-56	1.13E-57	1.13E-58	1.13E-59	1.13E-60	2.52E-61	2.52E-62	2.52E-63
700	4.12E-41	4.12E-42	4.12E-43	4.12E-44	4.12E-45	4.12E-46	4.12E-47	4.12E-48	4.12E-49	4.12E-50	4.12E-51	4.12E-52	8.17E-53	8.17E-54
800	6.31E-34	6.31E-35	6.31E-36	6.31E-37	6.31E-38	6.31E-39	6.31E-40	6.31E-41	6.31E-42	6.31E-43	6.31E-44	6.31E-45	6.31E-46	1.15E-46
900	2.52E-29	2.52E-29	2.52E-30	2.52E-31	2.52E-32	2.52E-33	2.52E-34	2.52E-35	2.52E-36	2.52E-37	2.52E-38	2.52E-39	2.52E-40	4.30E-41
1000	7.81E-24	7.81E-25	7.81E-26	7.81E-27	7.81E-28	7.81E-29	7.81E-30	7.81E-31	7.81E-32	7.81E-33	7.81E-34	7.81E-35	7.81E-36	7.81E-37
1100	3.76E-20	3.76E-21	3.76E-22	3.76E-23	3.76E-24	3.76E-25	3.76E-26	3.76E-27	3.76E-28	3.76E-29	3.76E-30	3.76E-31	3.76E-32	3.76E-33
1200	6.41E-14	4.48E-18	4.48E-19	4.48E-20	4.48E-21	4.48E-22	4.48E-23	4.48E-24	4.48E-25	4.48E-26	4.48E-27	4.48E-28	4.48E-29	4.48E-30
1300	3.47E-12	1.02E-12	1.82E-16	1.82E-17	1.82E-18	1.82E-19	1.82E-20	1.82E-21	1.82E-22	1.82E-23	1.82E-24	1.82E-25	1.82E-26	1.82E-27
1400	1.26E-10	3.14E-11	9.23E-12	3.17E-15	3.17E-16	3.17E-17	3.17E-18	3.17E-19	3.17E-20	3.17E-21	3.17E-22	3.17E-23	3.17E-24	3.17E-25
1500	2.24E-09	7.09E-10	1.81E-10	5.32E-11	2.81E-14	2.81E-15	2.81E-16	2.81E-17	2.81E-18	2.81E-19	2.81E-20	2.81E-21	2.81E-22	2.81E-23
1600	2.80E-08	8.84E-09	2.80E-09	7.23E-10	2.12E-10	1.43E-13	1.43E-14	1.43E-15	1.43E-16	1.43E-17	1.43E-18	1.43E-19	1.43E-20	1.43E-21
1700	2.60E-07	8.23E-08	2.60E-08	8.23E-09	2.13E-09	6.26E-10	1.63E-13	4.63E-14	4.63E-15	4.63E-16	4.63E-17	4.63E-18	4.63E-19	4.63E-20
1800	1.90E-06	6.00E-07	1.90E-07	6.00E-08	1.90E-08	4.89E-09	1.43E-09	1.03E-12	1.03E-13	1.03E-14	1.03E-15	1.03E-16	1.03E-17	1.03E-18

Table S4c. Equilibrium fraction of ① $\text{Ti}_{\text{Mg}}^{\times}$ doping type calculated with respect to temperature and oxygen partial pressure using surface model. (The equilibrium condition of H_2 and CO/CO_2 atmosphere is marked with green and blue lines.)

③ $\text{Ti}_{\text{Al}}^{\times} (\text{Ti}^{3+})$

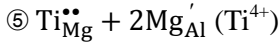
	1.00E-23	1.00E-21	1.00E-19	1.00E-17	1.00E-15	1.00E-13	1.00E-11	1.00E-09	1.00E-07	1.00E-05	1.00E-03	1.00E-01	1.00E+01	1.00E+03
100	6.47E-133	2.05E-133	6.47E-134	2.05E-134	6.47E-135	2.05E-135	6.47E-136	2.05E-136	6.47E-137	2.05E-137	6.47E-138	2.05E-138	6.47E-139	2.05E-139
200	7.24E-63	2.29E-63	7.24E-64	2.29E-64	7.24E-65	2.29E-65	7.24E-66	2.29E-66	7.24E-67	2.29E-67	7.24E-68	2.29E-68	7.24E-69	2.29E-69
300	8.48E-40	2.68E-40	8.48E-41	5.97E-41	1.89E-41	5.97E-42	1.89E-42	5.97E-43	1.89E-43	5.97E-44	1.89E-44	5.97E-45	1.89E-45	5.97E-46
400	5.70E-28	1.80E-28	5.70E-29	1.80E-29	5.70E-30	1.80E-30	5.70E-31	3.28E-31	1.04E-31	3.28E-32	1.04E-32	3.28E-33	1.04E-33	3.28E-34
500	7.45E-21	2.36E-21	7.45E-22	2.36E-22	7.45E-23	2.36E-23	7.45E-24	2.36E-24	7.45E-25	3.81E-25	1.20E-25	3.81E-26	1.20E-26	3.81E-27
600	4.27E-16	1.35E-16	4.27E-17	1.35E-17	4.27E-18	1.35E-18	4.27E-19	1.35E-19	4.27E-20	1.35E-20	4.27E-21	2.01E-21	6.36E-22	2.01E-22
700	1.09E-12	3.45E-13	1.09E-13	3.45E-14	1.09E-14	3.45E-15	1.09E-15	3.45E-16	1.09E-16	3.45E-17	1.09E-17	3.45E-18	1.54E-18	4.87E-19
800	4.00E-10	1.27E-10	4.00E-11	1.27E-11	4.00E-12	1.27E-12	4.00E-13	1.27E-13	4.00E-14	1.27E-14	4.00E-15	1.27E-15	4.00E-16	1.71E-16
900	4.01E-06	1.27E-08	4.01E-09	1.27E-09	4.01E-10	1.27E-10	4.01E-11	1.27E-11	4.01E-12	1.27E-12	4.01E-13	1.27E-13	4.01E-14	1.65E-14
1000	1.62E-06	4.11E-07	1.62E-07	5.11E-08	1.62E-08	5.11E-09	1.62E-09	5.11E-10	1.62E-10	5.11E-11	1.62E-11	5.11E-12	1.62E-12	5.11E-13
1100	3.36E-05	1.06E-05	3.36E-06	1.06E-06	3.36E-07	1.06E-07	3.36E-08	1.06E-08	3.36E-09	1.06E-09	3.36E-10	1.06E-10	3.36E-11	1.06E-11
1200	1.00E+00	3.14E-04	4.24E-05	1.34E-05	4.24E-06	1.34E-06	4.24E-07	1.34E-07	4.24E-08	1.34E-08	4.24E-09	1.34E-09	4.24E-10	1.34E-10
1300	1.00E+00	1.00E+00	3.65E-04	1.15E-04	3.65E-05	1.15E-05	3.65E-06	1.15E-06	3.65E-07	1.15E-07	3.65E-08	1.15E-08	3.65E-09	1.15E-09
1400	1.00E+00	1.00E+00	1.00E+00	7.35E-04	2.32E-04	7.35E-05	2.32E-05	7.35E-06	2.32E-06	7.35E-07	2.32E-07	7.35E-08	2.32E-08	7.35E-09
1500	1.00E+00	1.00E+00	1.00E+00	1.00E+00	1.16E-03	3.68E-04	1.16E-04	3.68E-05	1.16E-05	3.68E-06	1.16E-06	3.68E-07	1.16E-07	3.68E-08
1600	1.00E+00	1.00E+00	1.00E+00	1.00E+00	1.00E+00	1.51E-03	4.78E-04	1.51E-04	4.78E-05	1.51E-05	4.78E-06	1.51E-06	4.78E-07	1.51E-07
1700	1.00E+00	1.00E+00	1.00E+00	1.00E+00	1.00E+00	1.00E+00	1.67E-03	5.28E-04	1.67E-04	5.28E-05	1.67E-05	5.28E-06	1.67E-06	5.28E-07
1800	1.00E+00	1.61E-03	5.09E-04	1.61E-04	5.09E-05	1.61E-05	5.09E-06	1.61E-06						

Table S4d. Equilibrium fraction of ③ $\text{Ti}_{\text{Al}}^{\times}$ doping type calculated with respect to temperature and oxygen partial pressure using surface model. (The equilibrium condition of H_2 and CO/CO_2 atmosphere is marked with green and blue lines.)



	1.00E-23	1.00E-21	1.00E-19	1.00E-17	1.00E-15	1.00E-13	1.00E-11	1.00E-09	1.00E-07	1.00E-05	1.00E-03	1.00E-01	1.00E+01	1.00E+03
100	3.00E-161	9.50E-162	3.00E-162	9.50E-163	3.00E-163	9.50E-164	3.00E-164	9.50E-165	3.00E-165	9.50E-166	3.00E-166	9.50E-167	3.00E-167	9.50E-168
200	4.93E-77	1.56E-77	4.93E-78	1.56E-78	4.93E-79	1.56E-79	4.93E-80	1.56E-80	4.93E-81	1.56E-81	4.93E-82	1.56E-82	4.93E-83	1.56E-83
300	3.05E-49	9.63E-50	3.05E-50	2.14E-50	6.78E-51	2.14E-51	6.78E-52	2.14E-52	6.78E-53	2.14E-53	6.78E-54	2.14E-54	6.78E-55	2.14E-55
400	4.70E-35	1.49E-35	4.70E-36	1.49E-36	4.70E-37	1.49E-37	4.70E-38	2.71E-38	8.57E-39	2.71E-39	8.57E-40	2.71E-40	8.57E-41	2.71E-41
500	1.60E-26	5.07E-27	1.60E-27	5.07E-28	1.60E-28	5.07E-29	1.60E-29	5.07E-30	1.60E-30	8.20E-31	2.59E-31	8.20E-32	2.59E-32	8.20E-33
600	8.09E-21	2.56E-21	8.09E-22	2.56E-22	8.09E-23	2.56E-23	8.09E-24	2.56E-24	8.09E-25	2.56E-25	8.09E-26	3.81E-26	1.21E-26	3.81E-27
700	9.79E-17	3.10E-17	9.79E-18	3.10E-18	9.79E-19	3.10E-19	9.79E-20	3.10E-20	9.79E-21	3.10E-21	9.79E-22	3.10E-22	1.38E-22	4.36E-23
800	1.15E-13	3.64E-14	1.15E-14	3.64E-15	1.15E-15	3.64E-16	1.15E-16	3.64E-17	1.15E-17	3.64E-18	1.15E-18	3.64E-19	1.15E-19	4.91E-20
900	2.85E-11	9.01E-12	2.85E-12	9.01E-13	2.85E-13	9.01E-14	2.85E-14	9.01E-15	2.85E-15	9.01E-16	2.85E-16	9.01E-17	2.85E-17	1.18E-17
1000	2.37E-09	7.50E-10	2.37E-10	7.50E-11	2.37E-11	7.50E-12	2.37E-12	7.50E-13	2.37E-13	7.50E-14	2.37E-14	7.50E-15	2.37E-15	7.50E-16
1100	8.91E-08	2.82E-08	8.91E-09	2.82E-09	8.91E-10	2.82E-10	8.91E-11	2.82E-11	8.91E-12	2.82E-12	8.91E-13	2.82E-13	8.91E-14	2.82E-14
1200	4.35E-03	5.84E-07	1.85E-07	5.84E-08	1.85E-08	5.84E-09	1.85E-09	5.84E-10	1.85E-10	5.84E-11	1.85E-11	5.84E-12	1.85E-12	5.84E-13
1300	6.61E-03	6.61E-03	2.41E-06	7.63E-07	2.41E-07	7.63E-08	2.41E-08	7.63E-09	2.41E-09	7.63E-10	2.41E-10	7.63E-11	2.41E-11	7.63E-12
1400	9.47E-03	9.47E-03	9.47E-03	6.96E-06	2.20E-06	6.96E-07	2.20E-07	6.96E-08	2.20E-08	6.96E-09	2.20E-09	6.96E-10	2.20E-10	6.96E-11
1500	1.29E-02	1.29E-02	1.29E-02	1.29E-02	1.50E-05	4.75E-06	1.50E-06	4.75E-07	1.50E-07	4.75E-08	1.50E-08	4.75E-09	1.50E-09	4.75E-10
1600	1.69E-02	1.69E-02	1.69E-02	1.69E-02	1.69E-02	2.56E-05	8.09E-06	2.56E-06	8.09E-07	2.56E-07	8.09E-08	2.56E-08	8.09E-09	2.56E-09
1700	2.15E-02	2.15E-02	2.15E-02	2.15E-02	2.15E-02	2.15E-02	3.59E-05	1.14E-05	3.59E-06	1.14E-06	3.59E-07	1.14E-07	3.59E-08	1.14E-08
1800	2.67E-02	4.29E-05	1.36E-05	4.29E-06	1.36E-06	4.29E-07	1.36E-07	4.29E-08						

Table S4e. Equilibrium fraction of $\text{② Ti}_{\text{Mg}}^{\bullet} + \text{Mg}_{\text{Al}}' (\text{Ti}^{3+})$ doping type calculated with respect to temperature and oxygen partial pressure using surface model. (The equilibrium condition of H₂ and CO/CO₂ atmosphere is marked with green and blue lines.)



	1.00E-23	1.00E-21	1.00E-19	1.00E-17	1.00E-15	1.00E-13	1.00E-11	1.00E-09	1.00E-07	1.00E-05	1.00E-03	1.00E-01	1.00E+01	1.00E+03
100	4.93E-100													
200	2.22E-50													
300	7.90E-34													
400	1.49E-25													
500	1.38E-20													
600	2.81E-17													
700	6.51E-15													
800	3.86E-13													
900	9.24E-12													
1000	1.17E-10													
1100	9.38E-10													
1200	5.30E-09													
1300	2.30E-08													
1400	8.07E-08													
1500	2.40E-07													
1600	6.21E-07													
1700	1.44E-06													
1800	3.04E-06													

Table S4f. Equilibrium fraction of $\textcircled{5} \text{Ti}_{\text{Mg}}^{\bullet\bullet} + 2\text{Mg}_{\text{Al}}' (\text{Ti}^{4+})$ doping type calculated with respect to temperature and oxygen partial pressure using surface model. (The equilibrium condition of H₂ and CO/CO₂ atmosphere is marked with green and blue lines.)

S7. Surface formation energy for crystal models of each doping form

As discussed in S2, the surface formation energy can be calculated from the difference between energy of the surface crystal model and the corresponding bulk model. The difference comes from two main parts, cleaving and relaxation energy, which are related to the cleavage of the crystal by the insertion of a vacuum slab and relaxation of atomic position near the surface respectively. Table S5 lists the cleaving energy, the relaxation energy, and the surface formation energy of the surface crystal models, which contain various forms of Ti doping. The existence of Ti and point defects does not appear to affect the cleaving energy significantly, but the change in energy with surface relaxation for the ④ $\text{Ti}_{\text{Al}}^{\bullet} + \text{Mg}_{\text{Al}}'$ case was exceptionally large, resulting in lower surface energy than any other case of doping forms. This indicates that the doping of ④ $\text{Ti}_{\text{Al}}^{\bullet} + \text{Mg}_{\text{Al}}'$ near the surface is relatively stable; hence, the concentration of this form of doping is expected to be higher near the surface than in the bulk.

	ΔE_{cleave} (eV nm ⁻²)	ΔE_{relax} (eV nm ⁻²)	ΔE_{surf} (eV nm ⁻²)
MgAl ₂ O ₄ (without doping)	13.3512	-3.2970	10.0542
② $\text{Ti}_{\text{Al}}' + 0.5\text{V}_\text{O}^{\bullet\bullet}$	13.1442	-3.1181	10.0261
① $\text{Ti}_{\text{Al}}' + \text{Al}_{\text{Mg}}^{\bullet}$	12.0550	-2.9498	9.1051
① $\text{Ti}_{\text{Mg}}^{\times}$	12.2178	-2.6336	9.5842
③ $\text{Ti}_{\text{Al}}^{\times}$	12.7086	-3.6960	9.0127
② $\text{Ti}_{\text{Mg}}^{\bullet} + \text{Mg}_{\text{Al}}'$	12.7556	-3.7725	8.9830
④ $\text{Ti}_{\text{Al}}^{\bullet} + \text{Mg}_{\text{Al}}'$	13.2562	-4.3353	8.9209
⑤ $\text{Ti}_{\text{Mg}}^{\bullet\bullet} + 2\text{Mg}_{\text{Al}}'$	13.5926	-3.3385	10.2540

Table S5. Cleaving energy, relaxation energy, and surface formation energy of the (1 0 0) surface of Ti doped MgAl₂O₄ for various doping forms.

References

- s1 Y. Kim, H. Lee and S. Kang, *J. Mater. Chem.* 2012, **22**, 12874
- s2 L. Hu, Z. Xiong, C. Ouyang, S. Shi, Y. Ji, M. Lei, Z. Wang, H. Li, X. Huang and L. Chen, *Phys. Rev. B: Condens. Matter Mater. Phys.* 2005, **71**, 125433
- s3 P. W. Tasker, *J. Phys. C: Solid State Phys.* 1979, **12**, 4977
- s4 C. A. J. Fisher and M. S. Islam, *J. Mater. Chem.* 2008, **18**, 1209
- s5 M. S. Islam and C. A. J. Fisher, *Chem. Soc. Rev.* 2014, **43**, 185
- s6 D. A. Tompsett, S. C. Parker, P. G. Bruce and M. S. Islam, *Chem. Mater.* 2013, **25**, 536
- s7 C. A. J. Fisher and M. S. Islam, *J. Mater. Chem.* 2008, **18**, 1209
- s8 D. F. Shriver, P. W. Atkins, T. L. Overton, J. P. Rourke, M. T. Weller and F. A. Armstrong, *Inorganic Chemistry 4th edition*; Oxford university press: New York 2006